

Infrared Spectra of Cooling Flow Galaxies

W. Jaffe

Leiden Observatory, PO Box 9513, 2300RA Leiden, The Netherlands

M.N. Bremer

Department of Physics, Bristol University, H. H. Wills Laboratory, Tyndall Ave., Bristol, BS8 1TL, England

P.P. van der Werf

Leiden Observatory

Accepted 1988 December 15. Received 1988 December 14; in original form 1988 October 11

ABSTRACT

We have taken K-band spectra covering 7 cooling flow clusters. The spectra show many of the 1-0S transitions of molecular Hydrogen, as well as some of the higher vibrational transitions, and some lines of ionized Hydrogen. The line ratios allow us to conclude that the rotational states of the first excited vibrational state are in approximate LTE, so that densities above 10^5 cm^{-3} are likely, but there is evidence that the higher vibrational states are not in LTE. The lack of pressure balance between the molecular gas and the ionized components emphasizes the need for dynamic models of the gas. The ratios of the ionized to molecular lines are relatively constant but lower than from starburst regions, indicating that alternative heating mechanisms are necessary.

Key words: cooling flows – ISM:molecules – dust,extinction

1 INTRODUCTION

Cooling flows result when the hot, X-ray emitting, gas in a cluster is compressed by the gravitational force of the central galaxy to a density where it can cool in less than the Hubble time (c.f. Fabian 1994). In many cases 100-1000 M_{\odot}/yr condense out of the hot gas. They present at least two major unsolved problems: the ultimate fate of the gas after it has cooled, and the source of the copious optical line emission in the centre of the flows (Heckman et al. 1989, Voit and Donahue, 1997: VD97).

A new aspect of both these problems was revealed by the detection of infrared line emission of H_2 molecules from the centres of several CF clusters (Mouri 1994, Elston and Maloney 1994, Jaffe and Bremer 1997 (Paper I), Falcke et al. 1998, Genzel et al. 1998). This emission arises from dense gas at $\sim 2000 \text{ K}$ and is not found in similarly radio-loud AGNs not associated with CFs. Thus it represents *prima facie* evidence for “cool” material in cooling flows. Its spatial extent and energetics suggest an intimate association with the optical line emitting gas (Paper I). High surface brightness molecular line emission is generally concentrated within the giant central cluster galaxies (typically in the inner 10 kpc) in a similar manner to the emission from ionised gas. Both can be considered galactic-scale phenomena, even though the presence of the gas is statistically correlated with the presence of a cooling flow on larger scales (Paper I).

We do not yet understand the heating mechanism of the molecular gas, and cannot accurately estimate the mass associated with it. The mass in gas at 2000 K is only about $10^{5-6} M_{\odot}$ but the cooling time from this temperature is very short, about one year. Without a consistent thermal model, we do not know whether this represents a minor mass component (the equivalent of only 1000 years of CF mass accumulation) that is kept continually warm, or the tail of a cooler but much more massive molecular dog that is heated to IR temperatures by shocks, X-rays, or stellar photoionization.

In this paper we describe new K-band IR spectroscopy of six cooling flows taken with the United Kingdom InfraRed Telescope (UKIRT) on 2 and 3 January, 1997. By studying the ratios between the various lines of H_2 and between the H_2 and HII lines we hope to shed light on the thermal state of the gas, and ultimately on the heating mechanism. The clusters studied were Abell 0335, 478, 1795, and 2029, Hydra A, NGC 1275, and PKS 0745-19. They were observed with the CGS4 detector in the following configuration: 75 l/mm grating; 256(spectral) \times 84(spatial) InSb array; slit size:2”, spatial scale 1”/pixel, dispersion: .0026 μ /pixel.

2 OBSERVATION AND REDUCTION

The observations followed standard IR spectroscopic techniques. Each observation consists of a series of 60s frames,

consisting of four subframes, each shifted 1/2 pixel in the spectral direction. The four subframes are combined into a single 514x84 frame.

We calibrated the atmospheric transmission by observing, with the same technique, standard stars about every 90 minutes. We chose the stars from the Carlsberg Meridian Catalog (Fabricius, 1993) to be of early F type and within 10° of the target galaxies.

For any 1-dimensional target spectrum we used the telluric calibrators to subtract the smooth underlying stellar continuum leaving only non-atmospheric absorption and emission features. Our procedure is to find emission lines in these spectra, and then correct the fluxes for the atmospheric absorption, rather than to first correct the spectra and then fit lines. For narrow lines, the former procedure is less sensitive to spurious lines created by minor atmospheric fluctuations. These steps are illustrated for the cluster PKS0745-11 in Figure 1.

We applied this procedure to the summed 2-dimensional spectra for each cluster as follows: A continuum model, with atmospheric corrections, was subtracted from each row of the spectrum. This yields a 2-dimensional spectrum with emission/absorption lines only. We then summed the spatial profiles of the strongest hydrogen emission lines. The resulting profile was compared to the spatial profile of temporally adjacent standard stars to determine the spatial extent of the emitting regions. Lastly the rows of the 2-dimensional emission line spectrum were weighted by this spatial profile and summed to yield a single profile with the optimum signal/noise for detecting weak lines, assuming that all lines have the same profiles.

From the uncorrected spectra we determined, by gaussian fitting, the line widths of the strongest H_2 lines. We then searched for weaker lines by fitting gaussians of this given width at the given wavelengths of a large number of H_2 , HII, and metal lines. Because the position and width of the gaussians were fixed, the fitting procedure should have no bias toward finding positive peaks. We estimated the uncertainties in the fitted fluxes empirically by applying the same procedure at 100 random points along the spectrum and producing a smoothed r.m.s. average of the fluxes so determined as a function of wavelength. The method method includes residual atmospheric features and usually indicates a larger uncertainty in regions near strong telluric lines.

As a last step, the line strengths are converted to physical units by correcting for atmospheric absorption and using the standard star magnitudes. In this process an estimate of the uncertainty in the absorption is added in quadrature to the uncertainty in the gaussian estimate. The resulting flux and error estimates are given in Table 1 for each cluster except Abell 2029 where no lines were detected during 12 min of observation. The error estimates do not include the uncertainty of the absolute flux scale. This last uncertainty is relatively large because few of the Carlsberg calibrators have known K-band magnitudes, so their magnitudes were extrapolated to K-band from known B and R fluxes using a standard F-star spectrum. We estimate the additional uncertainty in the absolute line flux scale to be of order 30%, but the relative line strengths within one spectrum, or in one cluster relative to another, are accurate at the levels quoted in Table 1.

90

Figure 1 The top section shows the extracted spectrum and the best fitting continuum fit, including telluric absorption. The bottom section shows the difference – the uncorrected emission profile. Wavelengths are in the telescope system λ .

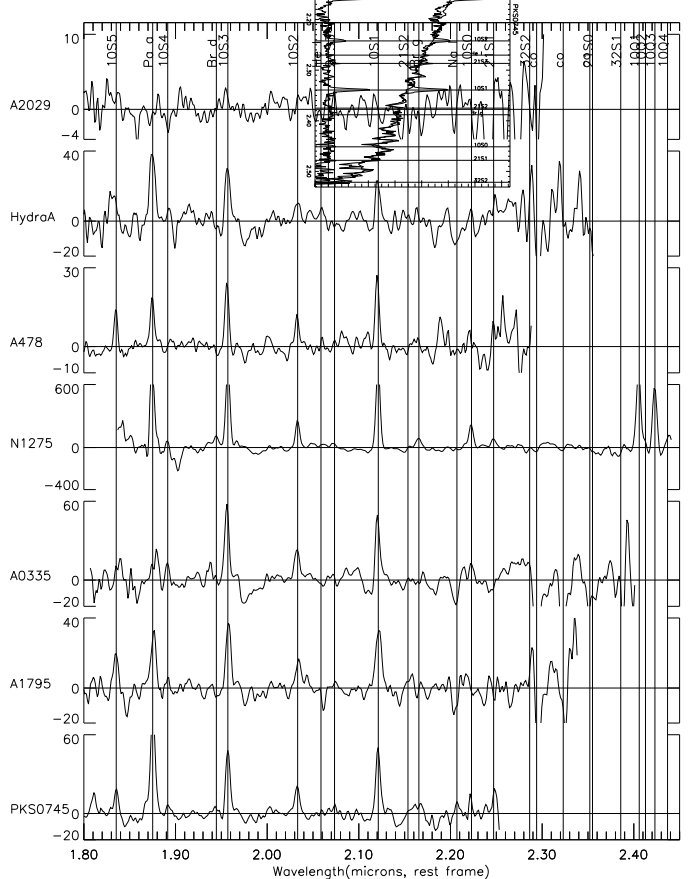


Figure 2. Calibrated and continuum subtracted spectra for the seven clusters studied. Wavelengths are in μ in the rest frame and the vertical scales are in $10^{-16} \text{ erg cm}^{-2} \text{ s}^{-1} \text{ \AA}^{-1}$

3 REDUCED SPECTRA AND DERIVED QUANTITIES

In Figure 2 we present the continuum subtracted and absorption corrected spectra for all clusters in physical units and in the rest wavelength frame. In Table 2 we present for

Table 1. Line fluxes from the studied clusters. Fluxes are in units of 10^{-16} erg cm $^{-2}$ s $^{-1}$.

Cluster	PKS0745	A0335	NGC1275	Abell 1795	Abell 478	Hydra A
Exposure Time (min)	60	54	12	30	100	56
z	0.1028	0.0349	0.0017	0.0616	0.0860	0.0540
1-0S(0) (2.2235 μ)	3.4 \pm 5.9	6.4 \pm 1.6	102.0 \pm 6.0	-0.6 \pm 1.4	2.4 \pm 1.4	3.7 \pm 1.3
1-0S(1) (2.1218 μ)	24.4 \pm 0.7	22.1 \pm 1.1	384.3 \pm 3.8	15.8 \pm 1.0	13.3 \pm 0.8	9.7 \pm 0.7
1-0S(2) (2.0338 μ)	9.2 \pm 0.6	9.9 \pm 0.8	115.1 \pm 6.2	7.4 \pm 0.6	5.9 \pm 0.6	3.1 \pm 0.6
1-0S(3) (1.9576 μ)	22.8 \pm 0.5	25.7 \pm 1.9	332.3 \pm 14.	17.4 \pm 0.4	12.0 \pm 0.4	15.5 \pm 1.6
1-0S(4) (1.1.8920 μ)	3.2 \pm 0.5	6.4 \pm 11.	59.2 \pm 28.	3.2 \pm 8.4	-1.4 \pm 0.8	2.9 \pm 4.3
1-0S(5) (1.8358 μ)	9.5 \pm 0.8	N.A.	N.A.	9.1 \pm 5.2	6.9 \pm 1.3	6.2 \pm 7.7
2-1S(1) (2.2477 μ)	7.2 \pm 6.0	-6.3 \pm 3.0	34.7 \pm 6.	-0.9 \pm 1.0	3.3 \pm 4.3	3.2 \pm 2.1
2-1S(2) (2.1542 μ)	1.4 \pm 0.8	-0.1 \pm 1.0	10.9 \pm 4.9	3.8 \pm 1.2	-1.6 \pm 0.7	1.3 \pm 0.9
2-1S(3) (2.0735 μ)	3.1 \pm 0.6	-0.4 \pm 0.8	13.1 \pm 3.6	2.6 \pm 0.9	0.5 \pm 0.7	-2.8 \pm 1.0
Pa α (1.8756 μ)	36.3 \pm 0.7	5.0 \pm 12.	300 ¹	14.0 \pm 3.1	8.4 \pm 0.6	17.6 \pm 1.3
Br γ (2.1661 μ)	3.7 \pm 0.8	-0.6 \pm 1.0	47.8 \pm 4.7	0.4 \pm 1.3	2.0 \pm 0.9	1.3 \pm 1.0
Br δ (1.9451 μ)	1.7 \pm 0.5	-2. \pm 12.	40.1 \pm 7.7	-1.7 \pm 1.0	-0.8 \pm 0.4	-1.8 \pm 1.9

¹ The Pa α line in NGC 1275 is clearly visible in Fig. 2, but lies in a region of strong and variable atmospheric absorption. The true line flux is highly uncertain.

each cluster the measured velocity dispersion of the brightest H $_2$ lines, the radial extent of the emission (standard deviation of gaussian fit along slit, deconvolved with stellar profile), the total luminosity in the detected H $_2$ lines the luminosity in Pa α , luminosity in H α (Heckman et al., 1989; White et al. 1994 for Abell 478) and the excitation temperature $T_{5,3}$, determined from the ratio of the 1-0S(3) and 1-0S(1) lines (c.f. Section 4.2). The instrumental dispersion, measured on arc and sky lines was 240 ± 10 km s $^{-1}$. This may be somewhat larger than the effective dispersion for emission that does not uniformly fill the slit. In comparing our luminosities with those of Heckman et al., determined by narrow band imaging, our luminosities should be corrected for light blocked by the slit jaws. This can be crudely estimated by assuming circular symmetry and calculating the light lost in this case from the emission profile along the slit. This leads to corrections ranging from 1.6 to 2, but these will be incorrect if the source is highly asymmetric, or if we have missed a very large, low brightness component. The latter possibility is particularly likely in the nearby cluster NGC 1275.

The velocity dispersions, corrected for instrumental widening, run from 100 to 300 km s $^{-1}$. These are comparable to the dispersions measured by Heckman et al. (1989) in H α and are much smaller than the typical velocities in the clusters, the stars in the envelopes of cD galaxies or gas in the narrow or broad line regions around active nuclei.

4 DISCUSSION

4.1 Optical Extinction

The ratio of H α to Pa α fluxes should measure the extinction of the optical light. This ratio, for Case B HII regions, should be about 7 (Osterbrock, 1989), and values much below this would indicate dust around the emission regions. Unfortunately the fluxes are measured with different techniques: slit spectroscopy for Pa α and narrow band imaging for H α . Hence the ratio is subject to uncertainties in the absolute calibration, and the flux lost outside of the spectroscopy slit. For the four high redshift clusters with good Pa α fluxes, we have taken the ratio $L_{H\alpha}/2L_{Pa\alpha}$, where the factor of 2 corrects for slit losses. The values of the ratio are

10, 22, 7, and 4, with an average of 11. While the variation confirms the difficulties with calibration, we conclude that there is no evidence for strong extinction of the H α fluxes (e.g. more than 1 magnitude).

4.2 LTE modelling of H $_2$ line ratios

If the warm gas is sufficiently dense that collisional transitions dominate over radiative transitions from the relevant states, then we can regard the gas to be in local thermal equilibrium (LTE). We regard this case as a reference model and ask if the measured line ratios are consistent with this model. In Table 2, we have given the excitation temperatures derived from the ratio of 1-0S(1) and 1-0S(3) lines; in Figures 3 we plot for each cluster $\log(F/ag)$ versus T_u . Here F is the measured flux in each line, and a , g and T_u are the Einstein coefficient, statistical weight and energy (expressed as a temperature, $T_u = E_u/k$) of the upper state of the transition. In LTE, of course, $\log(F/ag) = Constant - T_u/T$.

From Table 2 and Figure 3 we conclude that the LTE model is a reasonable approximation for the 1-0 lines in all clusters, with excitation temperatures of ~ 2000 K. There are some lines which deviate significantly more than the formal errors and these we have investigated individually. In some cases we have downgraded the significance of the result, because the line appears in a spectral region with a poor baseline. This is unfortunately true for many of the high excitation, but quite weak, 2-1 lines. By this standard, the remaining significant deviations from LTE are as follows:

For NGC 1275, the 2-1S(1) lies a factor of 3 above the LTE model for 1617 K. This is the cluster with the highest signal/noise ratios. Krabbe et al. (2000) discuss deeper observations of this object, where 2-1S(1),S(3) and 3-2S(3) are clearly detected. They find the higher lines to require higher excitation temperatures: 2600 K versus 1500K for the 1-0 lines) and attribute this largely to fluorescent excitation by Ly α photons. They conclude that for most transitions collisional processes dominate, requiring $n_e > 10^5$ cm $^{-3}$.

For A478 and PKS0745, and marginally for N1275 the 1-0S(4) line lies about a factor of 2 below the model.

Table 2. Quantities derived from analysis of the spectra.

Cluster	r(kpc)	σ_v (km s $^{-1}$)	L_{H_2} (erg s $^{-1}$)	$L_{Pa\alpha}$	$L_{H\alpha}$	$T_{5:3}$
PKS0745	1.5	320	$1.7 \cdot 10^{41}$	$7.3 \cdot 10^{40}$	$1.3 \cdot 10^{42}$	1771 ± 200
A0335	0.5 ¹	370	$1.5 \cdot 10^{40}$	N.A.	$5 \cdot 10^{41}$	2446 ± 900
NGC1275	0.13 ²	300	$6.1 \cdot 10^{38}$	N.A.	$2.1 \cdot 10^{41}$	1628 ± 100
Abell 1795	1.1	280	$4.2 \cdot 10^{40}$	$1.0 \cdot 10^{40}$	$4.4 \cdot 10^{41}$	2217 ± 350
Abell 478	1.8	260	$5.8 \cdot 10^{40}$	$1.2 \cdot 10^{40}$	$1.7 \cdot 10^{41}$	1693 ± 362
Hydra A	1.2	370	$2.3 \cdot 10^{40}$	$9.5 \cdot 10^{39}$	$7.2 \cdot 10^{40}$	${}^31480 \pm 300$

¹A0335—gaussian fit to spatial fit is poor. There is an unresolved core with $80 \pm 10\%$ of the flux. The remaining 20% extends to at least 3 kpc and has a gaussian fit radius of about 2 kpc. ²NGC 1275—gaussian fit is poor. Unresolved core with $\sim 85\%$ of flux. Remainder extends $\sim 10''$ or 3 kpc in radius. ³ see text at end of section 4.2

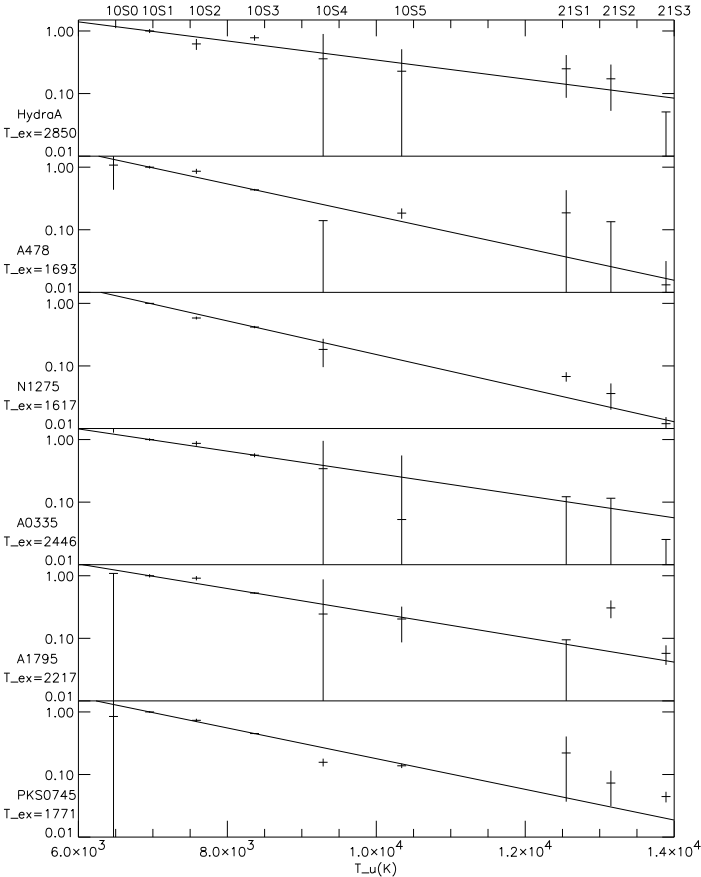


Figure 3. LTE Diagrams for the six clusters with detected lines. For each cluster the plot shows $\log F/ag$ vs. T_u with the straight line through the 1-0S(1) and 1-0S(3) points. For undetected lines, 2σ upper limits are given.

For Hydra A the ratio of 1-0S(3) to 1-0S(1) is so high (1.9) that no plausible excitation temperature can be assigned. This is probably due to the fact that the 1-0S(3) line falls in a telluric absorption band at 2.06μ and the correction for this is inaccurate. Excluding this line, the estimated excitation temperature for all the other 1-0S lines is 1480 ± 50 K

4.3 Physical Implications of the H $_2$ emission

We conclude from the above analysis that for the clusters studied the rotational states of the first excited vibrational state are close to LTE. This implies a gas density high enough that collisional transitions state dominate over radiative transitions. Using collision cross sections from Allison & Dalgarno (1967) and Sternberg & Dalgarno (1989), modified using more recent results by Mandy & Martin (1993), at $T = 2000$ K a molecular hydrogen density $n \geq 10^6$ cm $^{-3}$ is required for a 84% thermal population of the $v = 1, J = 7$ level which decays through the H $_2$ $v = 1 - 0$ S(5) line detected in A478 and PKS0745. For the remaining clusters, the highest line detected is H $_2$ $1 - 0$ S(3) which is 83% thermalized at $n = 3 \cdot 10^5$ cm $^{-3}$. Using collision cross sections from Le Boulrot et al (1999) would even increase these densities somewhat. On the other hand, if there is a significant electron abundance in the molecular gas, collisions with electrons would contribute to the excitation, decreasing the required densities. With a fractional ionization of 1%, the required densities would be decreased by a factor of two, for a fractional ionization of 10% the densities would be decreased by a factor of 10. Based on these considerations it is safe to conclude that the densities of the emitting regions are at least 10^5 cm $^{-3}$, and possibly even higher. At these densities, the line ratios provide little information on the gas heating source, since the signature of non-thermal excitation processes such as UV-pumping or X-ray excitation is quenched, except in lines of very high critical density which are faint and not detected in the present data.

The high density and temperature of the gas emitting the near-IR lines imply high thermal pressures ($nT \sim 10^{8-9}$ cm $^{-3}$ K), exceeding by of the order 100 to 1000 that of the X-ray gas in the region near the galaxy ($T \sim 10^7$, $n_e \sim 10^{-1}$) or the ionized optical line emitting gas ($T \sim 10^4$, $n_e \sim 10^2$) as estimated from the [SII] doublet ratio (Heckman et al., 1989). The latter two phases have comparable pressures. Because of this, most models of the *optical* line emission in the literature assume pressure equilibrium with the X-ray phase. Some theoretical work has been done on the expected properties of the molecular phase in cooling flows (e.g. Fabian 1994). Our results make it evident that a dynamic, non-isobaric model must be used to self-consistently explain the ionized and molecular line emission.

One possible model suggested by the obvious pressure imbalance, and the strong linkage of the optical and K-band fluxes, is an ablative or "rocket" model of the gas system. X- or UV-radiation could heat the surface layers of a cold,

gravitationally bound, molecular cloud to 2000 K. At this temperature the gas is no longer gravitationally bound and will expand into the surrounding space. As the density decreases the material will ionize and emit the observed optical line emission. We will explore this model, and test the predicted line ratios, in a future paper.

4.4 Relation of HII to H₂ emission

In general, the H₂ and HII emission in cooling flows are similarly distributed. As noted in Paper I, the H₂ and HII emission lines correlate well spatially, energetically, and kinematically. An extreme example of this is Abell 2029, which to date has shown no detectable H α or H₂ IR lines, although it is a strong cooling flow and strong radio source. In the two nearest clusters, NGC1275 and A0335, the IR line emission is dominated by an unresolved, presumably nuclear component. This is partly an artifact of their large angular size which excludes some of the extended emission from the slit. Both of these clusters have in fact, an extended component, as do the spectra of all of the other objects.

More recently, two of the objects in our sample were imaged with H₂ lines at high resolution with HST/NICMOS by Donahue et al., (2000). In the images, the H₂ emission traces H α emission. This implies that the H₂ and HII gas are cospatial on scales of a few hundred parsecs or less and strongly suggests that the excitation mechanisms of the two gas phases are either the same, or closely coupled.

For the four clusters in Table 2 for which good Pa α fluxes are available, the ratios of the ratios of $L_{H_2}/L_{Pa\alpha}$ range from 2.3 to 4.8 (mean=3.4). The single line ratio $L_{Pa\alpha}/L_{1-0S(1)}$ ranges from 0.6 to 1.8 (mean 1.0; rms 0.4). Br γ is generally not detected; the estimated ratio to 1-0S(1) is less than 0.15 in all cases.

The ratios of the HII lines to the H₂ lines are lower than those seen in “active” comparison galaxies: Seyferts, starburst galaxies and Ultraluminous InfraRed galaxies (ULIRGs). For all these galaxies, the ratio of Br γ /1-0S(1) is greater or equal than 1 (Moorwood & Oliva, 1988, 1990, Puxley et al., 1988, Genzel et al. 1995, Goldader et al., 1995, Thompson 1995, Vanzi et al., 1998, Genzel et al., 1998, Schinnerer et al., 1998, Murphy et al., 1999). We discuss the implications of this difference for UV-photoionization and shock excitation models below.

From the consistency of the line ratios, the spatial overlap, and the difference of the ratios from those of other active galaxies, we conclude that in most cooling flows the excitation of radiation from the ionized and molecular gas are causally related. This may not be true for some galaxies with exceedingly active nuclei. Cygnus-A for example shows a much higher ratio of Pa α /1-0S(1) than we find (Wilman et al., 2000).

4.5 Excitation by stellar UV radiation

Some authors (e.g. VD97) have suggested that the optical spectra of cooling flows can be explained largely by stellar photoionization. This cannot be the case for the molecular gas detected here. The faintness of Br γ in the cooling flows, compared to starburst galaxies, argues against H₂ excitation by star formation. Photo-ionization by the hottest stars is also known to be insufficient to account for the high electron temperatures in the ionized filaments of cooling flows,

which thus already required an additional source of excitation (VD97). The addition of the IR spectra to the optical spectra then potentially requires *three* excitation mechanisms to be acting simultaneously, and in concert, to yield the uniform IR spectra presented here.

An additional diagnostic is provided by the ortho/para ratio, which is expected to be three (the ratio of the statistical weights) in situations where the high-temperature equilibrium ortho/para ratio is reached (Burton et al. 1992). On the other hand, in regions where the H₂ lines are UV-excited, a significantly lower ortho/para ratio is expected, due to spin-exchange reactions with protons and hydrogen atoms (Draine & Bertoldi 1996). Indeed, a low ortho-para ratio is observed in the extended H₂ vibrational emission in the starburst galaxy NGC 253 (Harrison et al. 1998) and in regions of the well-studied Galactic photodissociation region in the Orion bar (Marconi et al., 1998) and the giant extragalactic HII region NGC 5461 (Puxley et al., 2000). The low ortho-para ratio in UV-excited regions has been highlighted in the models of Sternberg & Neufeld (1999).

In all of our targets, the $v = 1$ S(1) (ortho), S(2) (para) and S(3) (ortho) lines are detected at high signal-to-noise ratio and there is no indication for a deviation from a ortho/para ratio of three in our sample. Together with the above discussion, this argues against stellar UV-excitation.

4.6 Shock Excitation

A single shock model, where the various emission systems are produced in one gas stream that cools after the shock, does not predict the observed pressure differences between the HII and H₂ regions. A shock in cold gas, just strong enough to produce the 2000 K H₂ lines, would not produce the HII lines. A stronger shock could produce the HII lines, but, if the H₂ lines come from a cooler, post-shock region, the pressure there would be lower than directly behind the shock. A third alternative, a shock ionizing gas previously warmed to 2000 K, would also produce higher pressure in the HII gas than in the H₂ gas.

The consistent and low HII/H₂ line ratios severely restrict more complicated shock models. As discussed in paper I, only a narrow range of shock velocities, below ~ 30 km⁻¹, could produce the H₂ emission without excessive HII luminosity, while the characteristic velocities in the centers of cD galaxies are well above this. Van der Werf, et al. (1993) discuss a similar situation in the merging galaxy pair NGC 6240 (see further the section on LINERS below). They propose, effectively, that dense molecular clouds collide with a low density atomic or molecular ISM, forming a fast ionizing shock in the low density medium and a slow, C-type shock in the molecular medium. They do not explicitly calculate the ionized to molecular line ratios in this case, and we find the existence of such a low density, low temperature, medium unlikely at the centre of the cooling flow.

Alternatively, organized, rotation-like, motions of the cloud ensemble may allow the local cloud-cloud collisional velocities to be ~ 30 km⁻¹ while the large scale global motions are much higher. In this case the origin of the HII emission is unclear. It cannot arise directly in the shocks (because of the pressure argument) but might arise indirectly, for example in a star forming region downstream.

While the HII and H₂ line systems could conceivably

arise in different regions from different mechanisms (e.g. HII emission from a AGN narrow line region and H₂ lines from shocks in a circumnuclear disk), the low variation of the line ratios from cluster to cluster argues against unrelated emission sources.

We conclude that our results can be explained by systems of shocked clouds, but only under rather special conditions, whose likelihood requires further investigation.

4.7 Comparison to LINER spectra

The relative strengths of H₂(1-0)S(1) and Br γ in our spectra are remarkably similar to those found in LINER galaxies (e.g., Larkin et al., 1998), perhaps not surprisingly as the optical spectra of cooling flows also have many similarities with LINERS (e.g. VD97). Models for the excitation mechanisms in LINERS include central AGN photoionization and ionization by an aging starburst (effectively a mix of HII regions and supernova remnants, with a relative deficiency in ionizing photons accounting for the faintness of Br γ), and depend on the details of the near-IR spectrum (Alonso-Herrero et al., 2000). What produces the H₂ vibrational emission in LINERS is not clear, except in the class of LINERS where shock-excitation dominates the observed spectrum, e.g., in NGC6240, discussed above, which has an optical spectrum which is typical for shock-excited LINERS (e.g., Fosbury & Wall 1979, Fried & Schulz 1983, Heckman et al. 1987).

5 CONCLUSIONS

Our UKIRT observations detect multiple lines in six of the seven cooling flux clusters observed. In all cases except Abell 2029, we detect at least four of the 1-0S series, sometimes some of the 2-1S series. Paschen α is detected where the redshift allows this, but Br γ and δ are weak.

The ratio of molecular to ionized hydrogen line emission is much higher than those found in starburst regions or Seyfert galaxies, but are similar to those in LINERS. The ratios of H α to Pa α do not indicate large absorption of the former line by dust.

The 1-0S lines show near-LTE ratios, indicating densities well above 10⁵ cm⁻³. This implies pressures in the warm gas that are 2 to 3 orders of magnitude higher than the surrounding ionized gas, and rule out static equilibria.

The line ratio and pressure data argue against gas heating by stellar UV emission. X-ray heating in non-isobaric conditions remains an option, as do shocks under highly constrained conditions.

ACKNOWLEDGMENTS

UKIRT is owned by the United Kingdom Particle Physics and Astronomy Research Council and is operated by the British-Dutch-Canadian Joint Astronomy Centre at Hilo, Hawaii.

REFERENCES

Allen S. W., 1995, MNRAS, 276, 947
Allison A. C., Dalgarno A., 1967, Proc. Phys. Soc. London, 90, 609

Alonso-Herrero A., Rieke M.J., Rieke, G.H., Shields, J.C. 2000, ApJ, 530, 688
Burton, M.G., Hollenbach, D.J., Tielens, A.G.G.M. 1992, ApJ 399, 563
Donahue M., Mack J., Voit G.M., Sparks W., Elston R., Maloney P.R., 2000, astro-ph/0007062
Draine, B.T., Bertoldi, F. 1996, ApJ 468, 269
Elston R., Maloney P., 1994, in McLean I.S., ed. Infrared Astronomy with Arrays. Ap&SS Library, Vol. 190. Kluwer, Dordrecht, p. 169
Fabricius C., 1993, Bull. Inf. Centre Donnees Stellaires, 42, 5
Fabian A.C. 1994 ARA&A 32, 277
Falcke H., Rieke M.J., Rieke G.H., Simpson C., Wilson A.S., 1998, ApJ., 494, L115
Fosbury R. A. E., Wall J. V., 1979, MNRAS, 189, 79
Fried J. S., Schulz H., 1983, A&A, 118, 166 Genzel R., Weitzel L., Tacconi-Garman L.E., Blietz M., Cameron M., Krabbe A., Lutz D., Sternberg A., 1995, ApJ. 444, 129
Genzel R., Lutz, D., Strum E., Egami E., Kunze, D., Moorwood A.F.M., Rigopoulou D., Spoon H.W.W., Sternberg, A., Tacconi-Garman L.E., Tacconi L., Thatte N., 1998, Ap. J. 498, 579
Goldader J. D., Joseph F.D., Doyon R., Sanders D. B., 1995, ApJ., 444, 97
Harrison A., Puxley P., Russel A., Brand P., 1998, MNRAS, 297, 624
Heckman T.M., Armus L., Miley G. K., 1987, AJ, 93, 276
Heckman T. M., Baum S. A., Van Breugel W. J. M., McCarthy P., 1989, ApJ, 338, 48
Jaffe W., Bremer M. N., 1997, MNRAS, 284, L1 (Paper I)
Krabbe A., Sams B.J.III, Genzel R., Thatte N., Prada F., 2000, A&A 354, 439
Larkin J.E., Armus L., Knop R.A., Soifer B.T. Matthews K. 1998 ApJS, 114, 59
Le Bourlot J., Pineau Des Forets G., Flower D.R., 1999, MNRAS 305, 802
Marconi, A., Testi, L., Natta, A., Walmsley, C.M. 1998, AA 330, 69
Mandy M. E., Martin P. G., 1993, ApJS 86, 119
Moorwood A. F. M., Oliva E. 1988, A&A, 203, 278
Moorwood A. F. M., Oliva E. 1990, A&A, 239, 78
Mouri, H. 1994, Ap.J. 427, 777
Murphy T. W. Jr., Soifer B. T., Matthew K., Kiger J. R., Armus L., 1999, ApJ, 525, L85
Osterbrock D. E. 1989, Astrophys. of Gaseous Nebulae and Active Galactic Nuclei, University Science Books, Mill Valley CA.
Puxley, P.J., Hawarden, T.G., Mountain, C.M. 1988 MNRAS, 234, 29P
Puxley P.J., Ramsay Howat S.K., Mountain C.M. 2000, ApJ 529, 224
Schinnerer, E., Eckart A., Tacconi L.J. 1998, ApJ., 500, 147
Sternberg A., Dalgarno A. 1989, ApJ, 338, 197
Sternberg A., Neufeld D.A. 1999, ApJ, 516, 371
Thompson, R.I. 1995, ApJ, 445, 700
Van Der Werf P. P., Genzel R., Krabbe A., Blietz M., Lutz D., Drapatz S., Ward M. J., Forbes D. A., 1993, ApJ, 405, 522
Vanzi L., Alonso-Herrero A., 1998, ApJ, 504, 93
Voit G. M., Donahue M., 1997, Ap.J., 486, 242 (VD97)
Wilman R.J., Edge, A.C., Johnstone R.M., Crawford C.S., Fabian A.C., 2000 astro-ph 0007223
White D. A., Fabian A. C., Allen S. W., Edge A. C., Crawford C. S., Johnstone R. M., Stewart G. C., Voges W., 1994, MNRAS, 269, 589

This paper has been produced using the Royal Astronomical Society/Blackwell Science \TeX macros.